Transactions on Machine Intelligence 7(2) (2024) 147-160

ISSN Online: 2821-1693

Transactions on Machine Intelligence

Journal Homepage: https://tmachineintelligence.ir/

Designing Optimal Predictive Control Model for Boost Converter in Solar Inverters with the Help of Meta-Engineering Algorithms

D. Khalilzade[1,*], A. Ahrabi[2]

[1] Department of Electrical Engineering, K. N. Toosi University of Technology, Tehran 196976-4499, Iran
[2] Department of Electrical Engineering, K. N. Toosi University of Technology, Tehran 196976-4499, Iran

ARTICLE INFO

Article History:
Received 6 March 2024
Received in revised form 15 May 2024
Accepted 25 June 2024
Available online 30 June 2024

Keywords:
Predictive Model Control Design,
Boost Converter, Solar Energy

ABSTRACT

This study focuses on modeling the DC-DC converter and implementing predictive model control methods on the target system. The research aims to compare the efficiency of this approach against classical methods and devise a strategy for maximizing power extraction. Utilizing MATLAB software, we simulate the proposed converter and control method, analyzing the obtained data and results through comparison with alternative methods. The article aims to enhance the performance of the boost converter and DC-DC converter through predictive control. Specifically, the boost converter is tasked with converting 50 V photovoltaic voltage to 110 V. Our initial focus lies on designing predictive control for the boost converter, acknowledging its potential for higher accuracy compared to other control methods. However, a notable challenge of predictive control lies in manually determining coefficients in the cost function. In this work, we address this challenge by employing amplifying coefficients on the input and output of the MPC converter and determining these values using a meta-engineering algorithm. This approach aims to refine predictive control for improved performance. The proposed control demonstrates promising accuracy and speed in reaching set point values, with favorable energy metrics.

1. INTRODUCTION

The escalating demand for energy, coupled with rising fuel prices, global warming concerns, and a growing focus on environmental preservation, has led to increased interest in renewable energy sources[1-2]. Solar energy, wind, geothermal, and hydrogen (fuel cell) are among the many renewable options available, but solar energy stands out as a leading choice. Photovoltaic devices offer numerous advantages: they are environmentally friendly, emitting no pollution or noise, require no fuel costs, entail minimal maintenance, and most importantly, harness an essentially unlimited resource the sun's radiation. Just one hour of solar energy reaching the Earth equals the energy consumption of the entire global population for an entire year, underscoring their vast potential for large-scale deployment. Germany, for instance, witnessed a significant surge in solar energy adoption in 2010 alone, installing

* Corresponding Author: danial.khalilzade7710@gmail.com
Department of Electrical Engineering, K. N. Toosi University of Technology, Tehran 196976-4499, Iran

http://dx.doi.org/10.47176/TMI.2024.147

the equivalent of 7.4 gigawatts of solar electricity capacity, which is 1.4 times the total capacity of Iran's electricity network. This translates to over 30 million solar arrays installed[3-5]. Despite Germany and Japan receiving nearly half the solar radiation intensity compared to Iran, their total installed solar capacity in 2010 stood at 17.3, 3.7, 3.6, 3.5, and 2.5 gigawatts, respectively. The cost of photovoltaic power generation systems has significantly decreased over the past two decades, dropping from around $25 per kilowatt in 1980 to approximately $2 per kilowatt in 2010. This cost reduction has led to the widespread adoption of photovoltaic devices in various applications. In off-grid scenarios, these devices are commonly utilized in water pumps, street lighting, household appliances, battery chargers, and satellites. In grid-connected settings, they find use in hybrid devices and power plants. The control of DC-DC converters has been a focal point of research in recent decades, driven by the proliferation of electronic devices in daily life. The increasing demand for such appliances and equipment has spurred efforts to optimize their control mechanisms to enhance efficiency[6-9]. DC-DC converters have diverse applications, including use in laptops, photovoltaic systems, space systems, and fuel cells. The utilization of predictive model control in solar DC converters, particularly in DC-DC converters, represents a novel and highly effective approach for maximizing power output. This method facilitates the adjustment of voltage levels in photovoltaic modules, thereby enhancing energy extraction. For instance, boost converters can be employed to increase voltage levels, thereby optimizing power generation. The DC/DC converter serves to transform the input DC voltage level to a specified DC voltage level using a switching method. These converters can adjust the output voltage to be either lower or higher than the input voltage. Minimizing heat loss is crucial for efficient cooling operations, necessitating converters with low heat dissipation. Hence, advancements in power electronics have led to the development of PWM (Pulse Width Modulation) converters. These converters operate by modulating switches based on PWM pulses, allowing for precise control and regulation of the output voltage. PWM modulation finds applications not only in DC/DC converters but also in other types such as DC/AC and AC/AC converters.

2. BACKGROUND RESEARCH

Renewable energy sources, such as solar, wind, and sea waves, are typically smaller in scale compared to conventional power plants and are scattered around the distribution network. Consequently, they often contribute to the energy distribution sector. Solar energy generation is on the rise due to its advantages, particularly with the proliferation of electronic devices that utilize this clean energy source connected to the grid. However, connecting these energy generators to the grid poses new challenges, including managing the maximum power injected into the grid and enhancing system efficiency [10-14].One of the expanded control methods is the distributed energy resources control system, which aims to precisely adjust the output voltage of converters in the distributed energy resources system to the desired reference. A non-linear adaptive controller is designed for controlling this system. Using the Lyapunov method, the controller pursues the control objectives. Simulation results indicate that the controller successfully achieves its control goal to a satisfactory degree when dealing with load and fuel changes that lead to variations in input voltage. Nevertheless, a limitation is noted, as the controller is unable to operate outside the rated range [15]. The author employs the sliding mode control method (SMC) adaptively to handle load changes and unknown input voltage. These controllers demonstrate good resistance to bounded uncertainties. However, a drawback is observed in the form of chattering behavior near the slip point [16]. Among the array of proposed methods is the integration of various neural, fuzzy, and adaptive control techniques into a network known as AFNNC (Adaptive Fuzzy Neural Network Controller). AFNNC is deployed to regulate the boost converter. This approach notably mitigates the chattering phenomenon associated with the traditional tsmc control method, eliminating the necessity for intricate system dynamics details and compensation via auxiliary controllers [17]. In [18], two distinct maximum power point tracking methods for photovoltaic systems are introduced. The first method employs an intelligent algorithm based on a fuzzy logic controller, while the second method adopts a conventional disturbance and observation structure. Results indicate that the first method exhibits superior dynamic performance and yields higher power output compared to the perturbation and observation algorithm. In[19] a maximum power point tracking controller design is outlined for single-phase and two-phase grid-connected photovoltaic systems, leveraging an adaptive fuzzy controller. Findings demonstrate that the controller efficiently reaches the maximum power point with reduced and quicker fluctuations. Consequently, system efficiency is enhanced, fluctuations are minimized, and the quality of output power in single-phase and two-phase systems is improved. In [20], the focus lies on studying and comparing various methods for tracking the maximum power point to evaluate power extraction under standard test conditions and varying weather conditions. Results indicate that the fuzzy controller algorithm

achieves a stabilization time of 5 ms in terms of response time, with minimal fluctuation observed around the operating point.

3. PREDICTIVE CONTROL STRATEGY

Predictive control, or model-based predictive control, encompasses a group of computer control algorithms with shared characteristics, rather than referring to a specific controller.

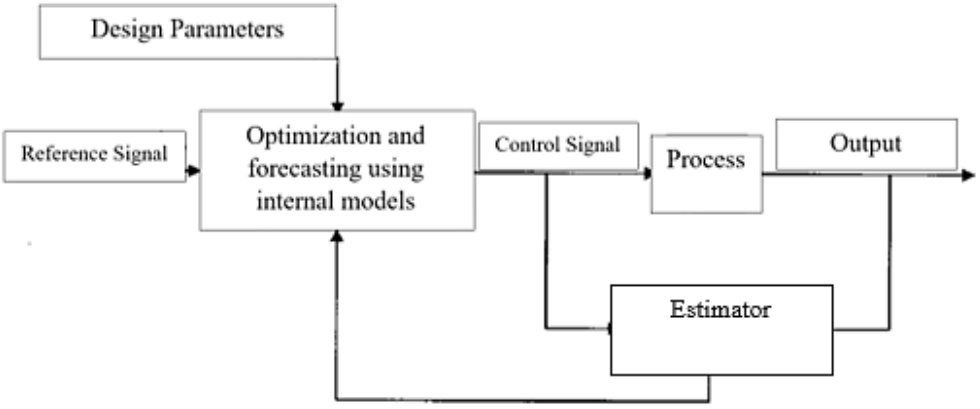

Fig. 1. Predictive control block diagram [37]

The predictive control block diagram, as depicted in Figure [21], embodies three key characteristics: Utilization of Process Model: Predictive control relies on the process model to forecast its future behavior. Solving an Optimization Problem: The controller tackles an optimization problem to determine the optimal control actions. Receding Horizon Approach: A series of computed signals, typically involving the "first element," are implemented in the process. This sequence of steps repeats during subsequent sampling intervals.

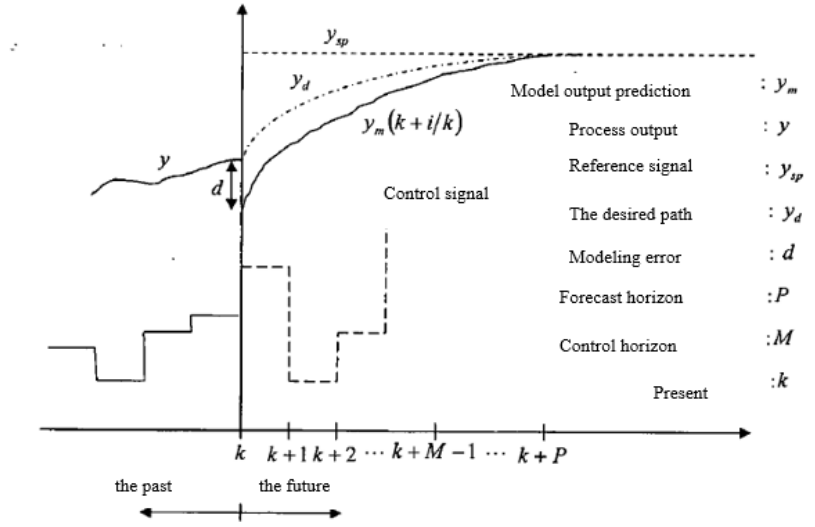

Fig. 2. The figure shows how predictive control works. [21]

As depicted in the figure, predictive control aims to determine future inputs, denoted as M, in a manner that minimizes the error between predicted future outputs and their desired trajectory over a defined time interval, such as "P sample". Achieving this objective requires a model alongside the process, enabling the prediction of the process output behavior by applying future inputs. Subsequently, this prediction should closely align with the desired trajectory. To accomplish this, a cost function needs definition, and the optimization problem must be solved.

Consequently, predictive control entails four actions in each sampling period: Calculation of Desired Path: From the reference signal and the current process output, compute the desired trajectory. Prediction of Future Outputs: Utilizing the model, forecast future output values. Notably, these future output values are contingent upon the future input values, necessitating calculation by the optimization algorithm. Minimization of Cost Function: Minimize the cost function, encompassing future errors and changes in control signals. Application of Control Signal: Implement the first calculated control signal value onto the process, repeating calculations with new information for the subsequent sampling period. In predictive control, it is assumed that after several steps, the control signal changes equal to zero. That is:

$$\delta u(t+i) = 0 \quad i \geq M \tag{1}$$

In the cost function, assigning an infinite weight to control signal changes from a certain time onward implies prioritizing stability and minimizing fluctuations in control actions. For instance, if M equals one, only one control change is factored into the cost function, with all subsequent values of u(k+i) regarded as equal to u(k). Decreasing the value of M enhances the convergence speed of the optimization algorithm since it reduces the number of variables requiring optimization. This approach streamlines the optimization process by focusing on fewer variables, thereby accelerating convergence toward an optimal solution. One fundamental parameter in predictive control is the prediction horizon, representing the number of periods over which the controller endeavors to minimize the discrepancy between the output and the reference trajectory. Typically, there exists a maximum value for the prediction horizon, beyond which further increments do not yield discernible enhancements in controller performance. In practical applications, an optimal prediction horizon value often aligns closely with the rise time of the process in open-loop mode. For non-minimum phase processes characterized by an initial negative slope response, it becomes imperative to extend the prediction horizon sufficiently to encompass output samples exhibiting positive slopes within the cost function. Initially, predictive control is designed for the system, following which the designed predictive control undergoes optimization using a meta-engineering algorithm. The design phase focuses on formulating predictive control, while subsequent discussions delve into optimizing the designed predictive control. Predictive Controller in Unrestricted Mode: In the initial phase, it's imperative to formulate the boost converter using state equations.

$$\begin{aligned}
&\dot{x}(t) = \left(u(t)A_{c1} + \left(1-u(t)\right)A_{c2}\right)x(t) + \left(u(t)B_{c1} + \left(1-u(t)\right)B_{c2}\right)v(t) \\
&A_{c1} = \begin{bmatrix} -\frac{R_{no}}{L} & 0 \\ 0 & -\frac{1}{RC} \end{bmatrix} \qquad A_{c2} = \begin{bmatrix} 0 & \frac{-1}{L} \\ \frac{1}{C} & \frac{-1}{RC} \end{bmatrix} \\
&B_{c1} = \begin{bmatrix} \frac{1}{L} & 0 \\ 0 & 0 \end{bmatrix} \qquad B_{c2} = \begin{bmatrix} \frac{1}{L} & \frac{-1}{L} \\ 0 & 0 \end{bmatrix}
\end{aligned} \tag{2}$$

By defining the matrices

$$\begin{aligned}
B_c &= \left(B_{c1} - B_{c2}\right)v \\
G_c &= A_{c1} - A_{c2}
\end{aligned} \tag{3}$$

The discrete equations of the system will be obtained as follows.

$$\begin{aligned}
&x(k+1) = A_2 x(k) + \left(B + Gx(k)\right)u(k) + B_2 v(k) \\
&A_2 = hA_{c2} + I, \quad B = hB_c, \quad G = hG_c, \quad B_2 = hB_{c2}
\end{aligned} \tag{4}$$

Then the value and the value are also from the relation will be calculated. Among these two values, one is chosen that corresponds to the value calculated from the following equation.

$$x_2^0 = \frac{-\alpha_1 \pm \sqrt{\alpha_1^2 - 4\alpha_0\alpha_2}}{2\alpha_2}$$
$$u^0 = \frac{(1-a_{21})r_I - a_{22}x_2^0 - b_{21}v_g - b_{22}v_D}{b_1 + g_1 r_I + g_2 x_2^0} \quad (6)$$

Also in high relations:

$$\alpha_0 = -\left(a_{23}r_I + b_{23}v_g + b_{24}v_d\right)\left(b_1 + g_1 r_I\right) - \left(\left(1-a_{21}\right)r_I - b_{21}v_g - b_{22}v_d\right)\left(b_2 + g_3 r_I\right)$$
$$\alpha_1 = \left(b_1 + g_1 r_I\right)\left(1-a_{24}\right) - \left(a_{23}r_I + b_{23}v_g + b_{24}v_d\right)g_2 + a_{22}\left(b_2 + g_3 r_I\right) \quad (7)$$
$$-\left(\left(1-a_{21}\right)r_I - b_{21}v_g - b_{22}v_d\right)g_4$$
$$\alpha_2 = \left(1-a_{24}\right)g_2 + a_{22}g_4$$

It will be calculated from the above relations. Then the matrix T from the relation:

$$T = B + Gx^0 \quad (8)$$

calculated and the vector will also be calculated from the following relationship.

$$e_x = x(k) - x^0 \quad (9)$$

By choosing the matrix and as

$$P_c = \begin{bmatrix} 0.0016 & 0 \\ 0 & 0.001 \end{bmatrix} \quad (10)$$
$$\rho = 0.01$$

The control signal will be calculated from the relationship. This function receives inputs from simulink and calculates the control signal. Now we describe the Similink file.

$$u_{ur}^* = \frac{-c_1(e_x) + 2\rho u^0}{2\left(c_2(e_x) + \rho\right)}$$
$$c_1(e_x) = 2\left(T + Ge_x\right)^T P_c\left(A_2 e_x - Tu^0\right) \quad (11)$$
$$c_2(e_x) = \left(T + Ge_x\right)^T P_c\left(T + Ge_x\right)$$

4. SIMULATION

This function receives inputs from simulink and calculates the control signal. Now we describe the Similink file.

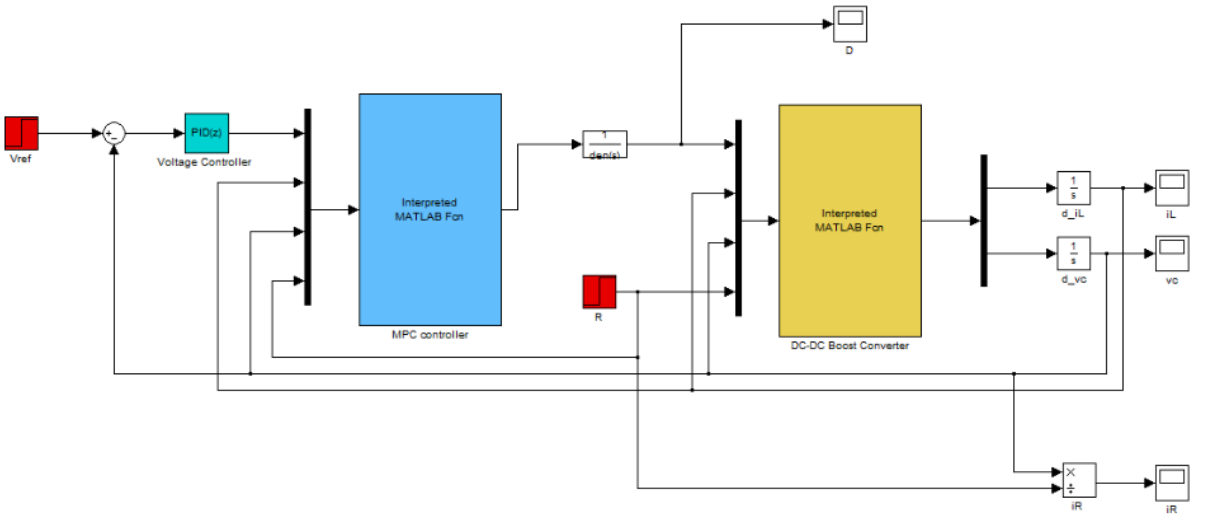

Fig. 3. Schematic figure of the simulation

In the provided function, derivative values are computed internally, while integration is performed externally to the block. For this simulation, the load value is set at 50 ohms, which can be adjusted as needed. Assuming a reference voltage of 67 volts for the initial 1 second, followed by a transition to 100 volts, the simulation yields the following results:Figure output voltage and reference value The shape of the control signal If the reference voltage changes from 67 to 120 volts, the simulation results are obtained as follows.

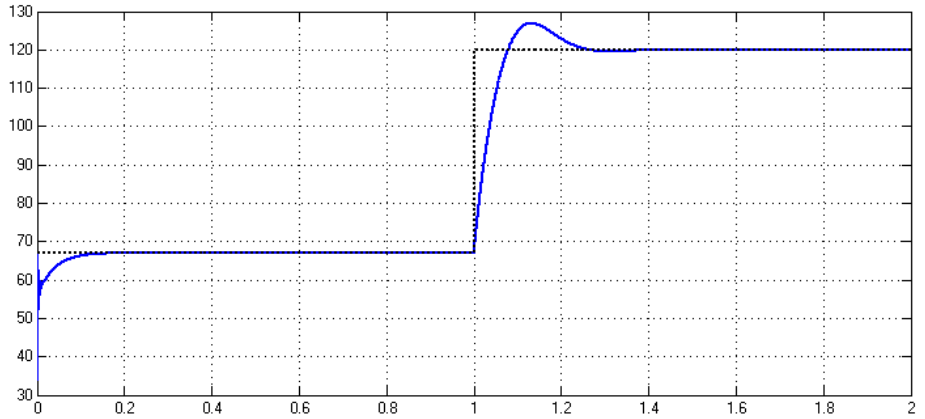

Fig. 4. Output Voltage and Reference Value

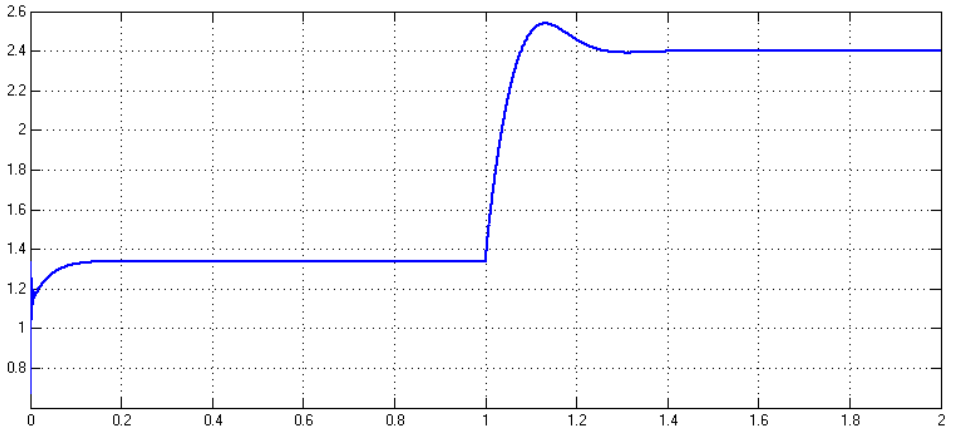

Fig. 5. Output voltage figure

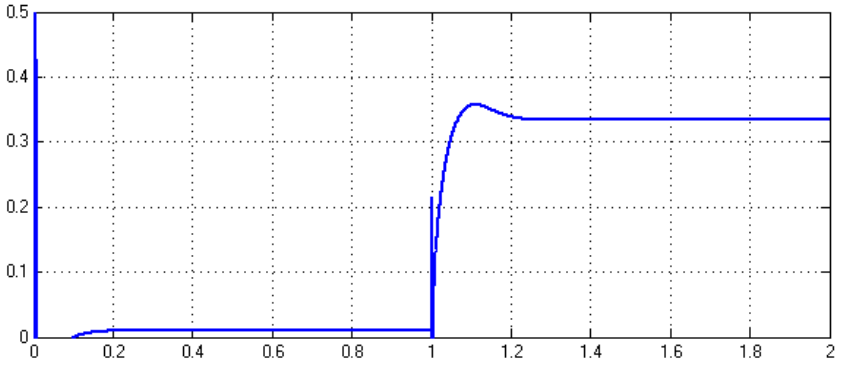

Fig. 6. The shape of the control signal

If the reference voltage is 67 and the load resistance changes from 75 to 37.5, the simulation results will be as shown below.

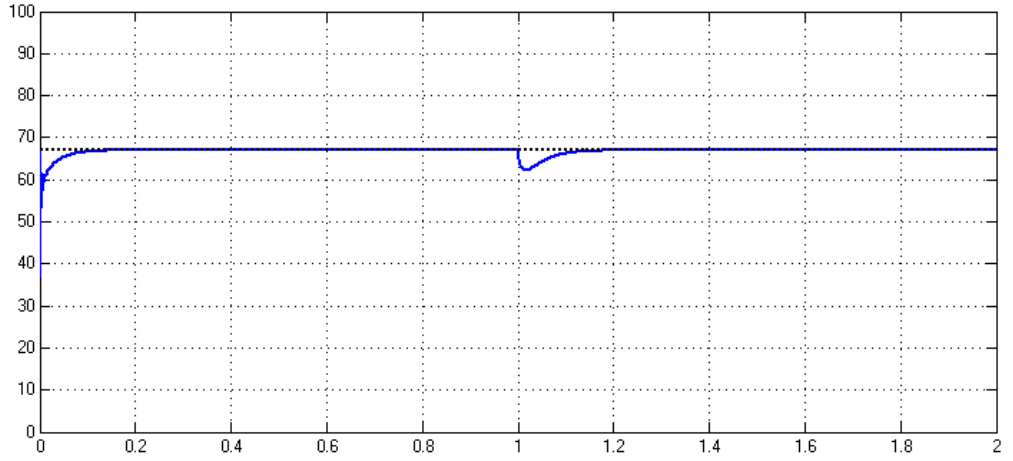

Fig. 7. Output voltage figure

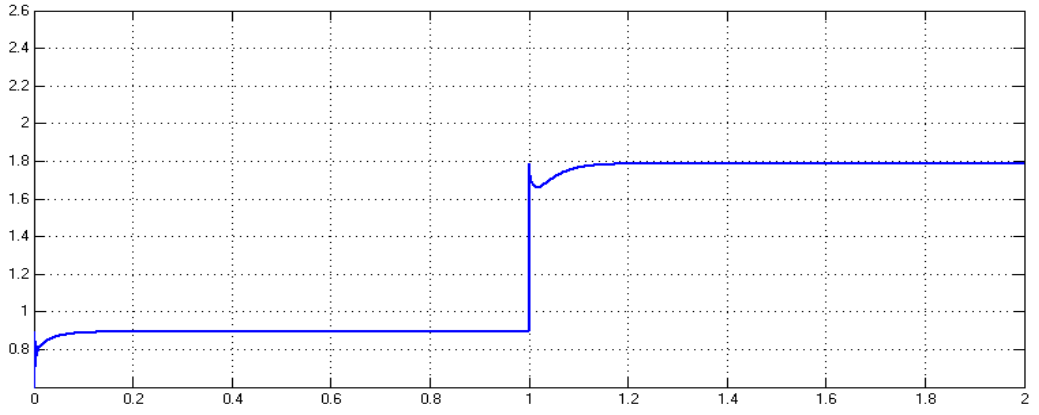

Fig. 8. Load flow shape

Predictive controller in limited mode: In this case, the control signal should be calculated considering the following limitations

$$\begin{aligned} &D_{\min} \le D \le D_{\max} \\ &0 \le i_L(k) \le 5 \\ &0 \le v_c(k) \le 150 \end{aligned} \tag{12}$$

The simulation environment for the boost converter, incorporating predictive control, is outlined below. To enhance control performance and minimize controller energy consumption, two coefficients are incorporated into the input and output of the MPC (Model Predictive Control) system. These coefficients are determined by a meta-engineering algorithm.

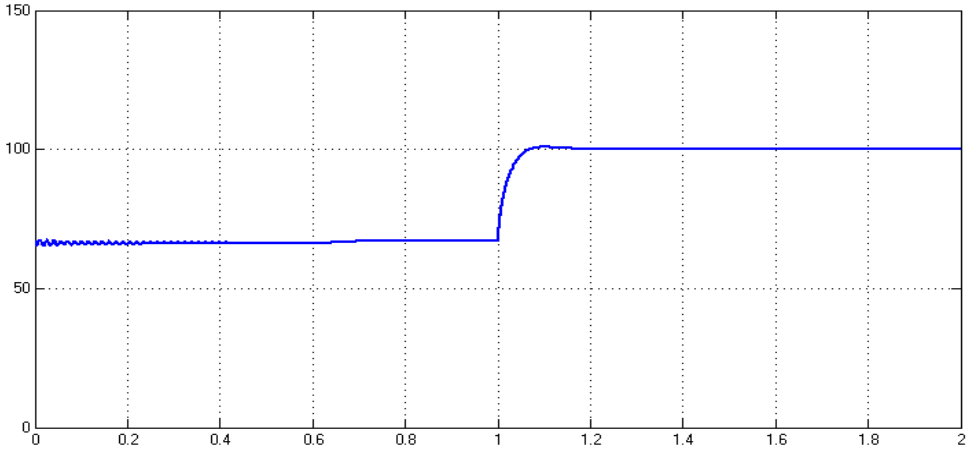

Fig. 9. The Output Voltage for The Limited Mode

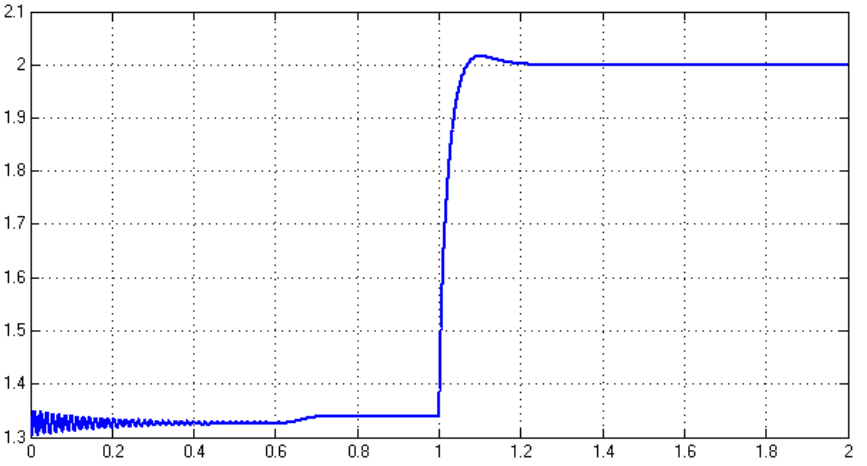

Fig. 10. The Output Current for The Constrained Mode

After applying predictive control, the simulation environment integrates the boost converter with the inverter. This setup ensures that the control system operates optimally while effectively managing energy consumption. The simulation environment in MATLAB is considered as follows. The shape of the simulation environment in the MATLAB environment along with the boost converter

5. DETERMINING THE OPTIMAL COEFFICIENTS OF THE CONTROLLER

In the preceding section, predictive control is explored across various modes, with coefficients introduced into the control section. Additionally, the meta-engineering algorithm aids in determining these coefficients, which contribute to minimizing permanent errors in the control system. The shape of the boost converter along with the optimized coefficients with the meta-engineering algorithm To determine the coefficients, the cuckoo algorithm will

be employed. In this algorithm, the energy cost is formulated as a function of the system error, allowing both factors to be optimally minimized simultaneously. The cuckoo algorithm operates as follows:

Table 1. Tuning parameters for the cuckoo algorithm

Cuckoo Algorithm Indicators	Amounts
numCuckooS	5; % number of initial population
minNumberOfEggs	2; % minimum number of eggs for each cuckoo
maxNumberOfEggs	4; % maximum number of eggs for each cuckoo
maxIter	100; % maximum iterations of the Cuckoo Algorithm
knnClusterNum	1; % number of clusters that we want to make
motionCoeff	9; % Lambda variable in COA paper, default=2
accuracy	-inf; % How much accuracy in answer is needed
radiusCoeff	5; % Control parameter of egg laying
cuckooPopVariance	1e-13; % population variance that cuts the optimization

Upon executing the cuckoo algorithm, the cost function undergoes reduction as depicted below. The reduction of the cost function is illustrated in terms of the number of iterations. Cuckoo algorithm optimization form and cost function reduction Following optimization, the first step involves examining the voltage diagram of the boost converter. We anticipate that the voltage will closely track the set value and rapidly reach the desired value.

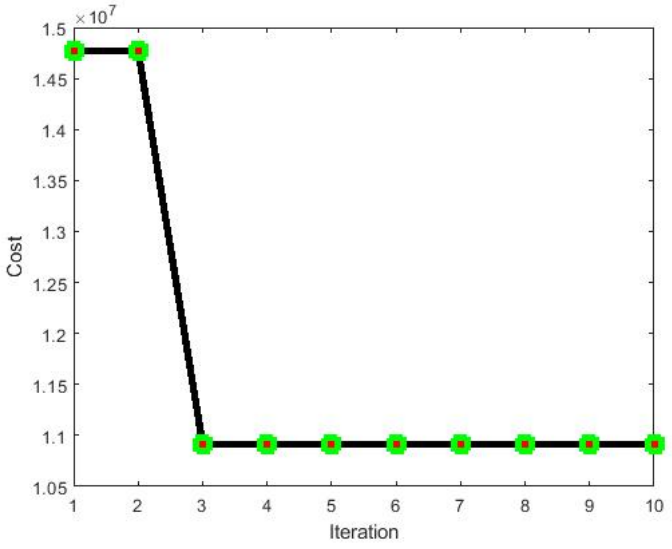

Fig. 11. Cuckoo algorithm optimization form and cost function reduction

After the optimization, we first check the voltage diagram of the boost converter, which we expect to follow the set value and reach the desired value in the shortest time.

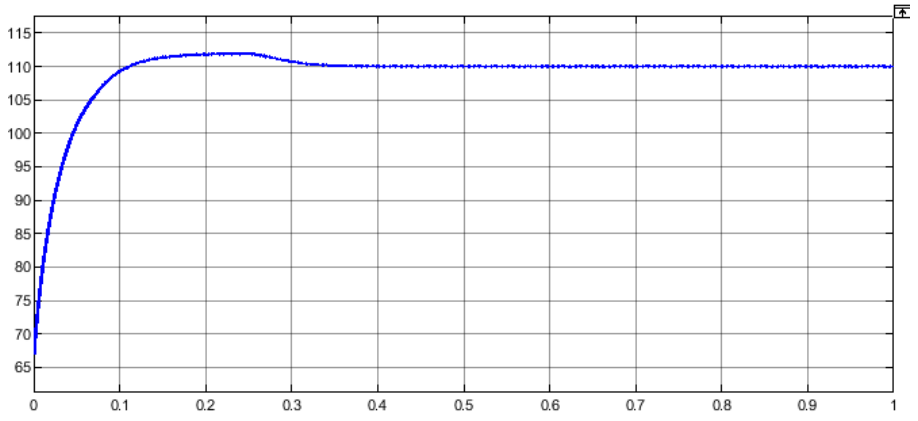

Fig. 12. the voltage value of the boost converter with the help of coefficients optimized by the cuckoo algorithm

The network voltage and current are as follows:

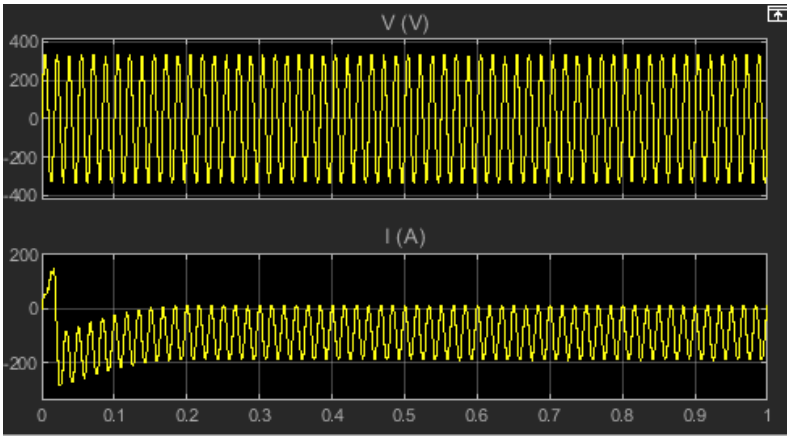

a: network voltage and current

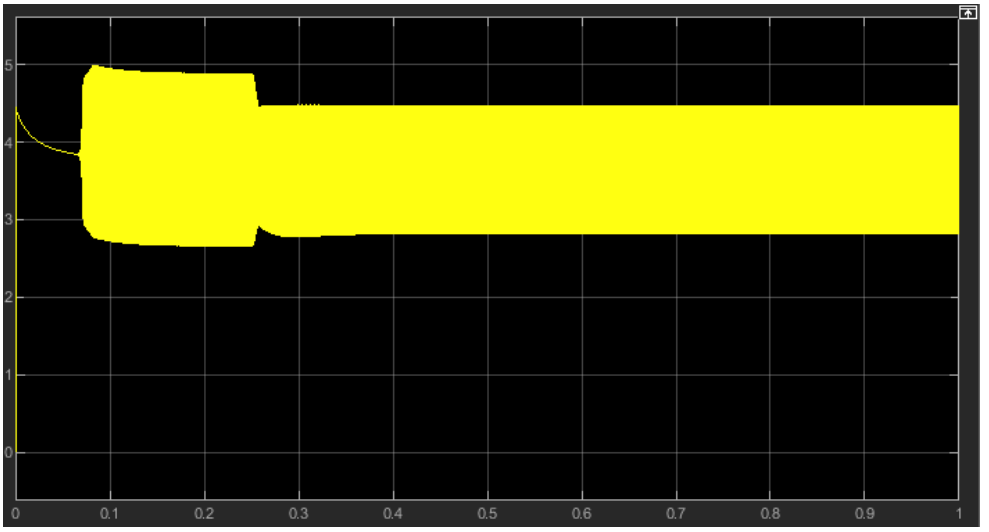

b: load flow

Fig. 13. System Simulation Using Pid Control

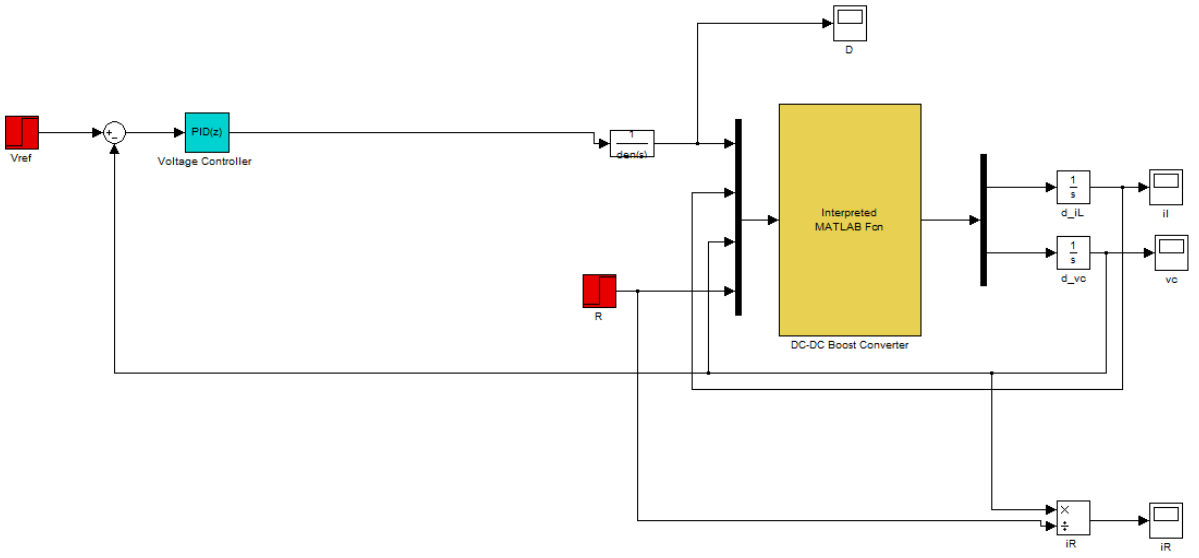

Fig. 14. Simulation and Simulink using pi controller

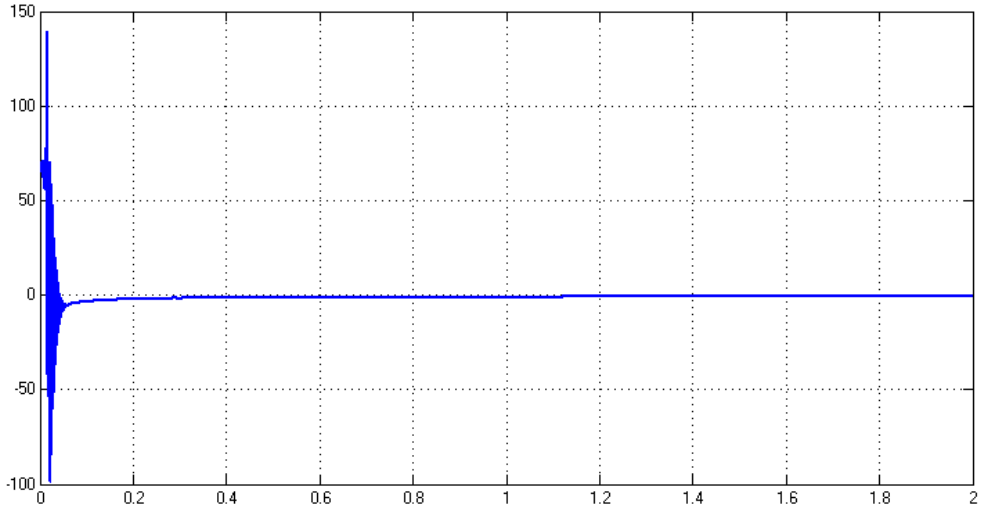

Fig. 15. The value of il after simulation

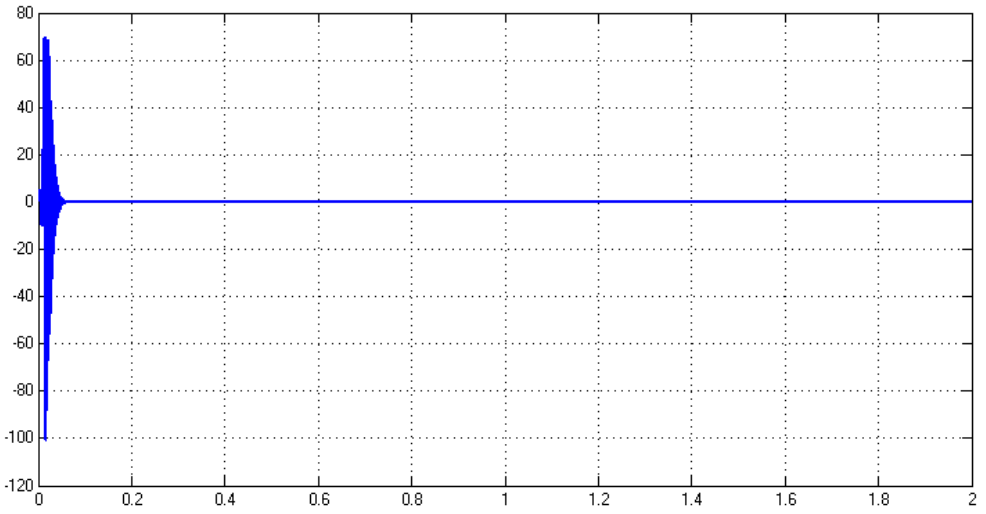

Fig. 16. the simulated vc value

As you can see, pi control has not been able to bring the voltage and current values to their final value.This article focuses on enhancing the performance of a boost converter and a DC-to-DC converter through advanced control techniques. Specifically, the boost converter under consideration aims to convert a photovoltaic voltage of 50 volts to 110 volts. The initial approach involves designing predictive control for the boost converter. While predictive control offers superior accuracy compared to other control methods, it poses a challenge in manually determining coefficients in the cost function. To address this challenge, the article proposes the use of amplifying coefficients on the input and output of the MPC (Model Predictive Control) converter. These coefficients are then determined using a meta-engineering algorithm, thereby improving predictive control. The results, as depicted in the accompanying graphs, demonstrate that the proposed control strategy exhibits excellent accuracy and speed in reaching set point values. Moreover, energy consumption values also indicate favorable outcomes, showcasing the effectiveness of the proposed approach.

6. CONCOLUSION

In this paper, we investigated methods for eliminating physiological hand tremors in minimally invasive robotic surgery technology. The Kalman filter was capable of optimally removing this involuntary tremor as noise from intentional hand movements, assuming its variance remained constant and predetermined. However, in physiological tremors, the variance of the tremor is time-varying and cannot be determined at a fixed value during the estimation update phase. Therefore, we introduced an adaptive Kalman filter in which the measurement variance was adaptively adjusted. We employed two methods for this purpose. First, we designed a fuzzy inference system, and due to the availability of prior knowledge, achieved a satisfactory solution for tremor elimination. The second method involved Q-learning, where the agent, through exploration in the state-action space, autonomously reached an optimal policy for estimating tremor variance.

Declaration

We acknowledge that we used ChatGPT to enhance the academic writing of our manuscript while ensuring the originality and integrity of our work.

Transparency Statement

The data supporting this study are available upon reasonable request to the corresponding author, subject to ethical and confidentiality considerations.

Acknowledgments

We would like to express our gratitude to all individuals who contributed to this project.

Declaration of Interest

The authors declare that they have no competing interests.

Funding

This research received no specific grant from any funding agency, commercial, or not-for-profit sectors.

REFERENCE

[1] Rego, R., & Costa, M. (2020). Output feedback robust control with anti-windup applied to the 3SSC boost converter. IEEE Latin America Transactions, 18(5), 874–880. https://doi.org/10.1109/TLA.2020.9082915

[2] Wahlström, J., & Eriksson, L. (2012). Output selection and its implications for MPC of EGR and VGT in diesel engines. IEEE Transactions on Control Systems Technology, 21(3), 932–940. https://doi.org/10.1109/TCST.2012.2191289

[3] Hammons, T. (Ed.). (2009). Renewable energy. BoD–Books on Demand.

[4] Cabrera-Tobar, A., Bullich-Massagué, E., Aragüés-Peñalba, M., & Gomis-Bellmunt, O. (2016). Review of advanced grid requirements for the integration of large scale photovoltaic power plants in the transmission system. Renewable and Sustainable Energy Reviews, 62, 971–987. https://doi.org/10.1016/j.rser.2016.05.044

[5] Gevorgian, V., & Booth, S. (2013). Review of PREPA technical requirements for interconnecting wind and solar generation (NREL/TP-5D00-57089). National Renewable Energy Laboratory. https://doi.org/10.2172/1260328

[6] Lappalainen, K., & Valkealahti, S. (2020). Experimental study of the behaviour of the global MPP of partially shaded PV strings. In Proceedings of the 37th European Photovoltaic Solar Energy Conference (pp. 1501–1505). https://doi.org/10.4229/EUPVSEC20202020-5CV.3.4

[7] Marcos, J., Marroyo, L., Lorenzo, E., Alvira, D., & Izco, E. (2011). Power output fluctuations in large scale PV plants: One year observations with one second resolution and a derived analytic model. Progress in Photovoltaics: Research and Applications, 19(2), 218–227. https://doi.org/10.1002/pip.1016

[8] Lappalainen, K., & Valkealahti, S. (2017). Output power variation of different PV array configurations during irradiance transitions caused by moving clouds. Applied Energy, 190, 902–910. https://doi.org/10.1016/j.apenergy.2017.01.013

[9] Chen, X., Du, Y., Lim, E., Wen, H., Yan, K., & Kirtley, J. (2020). Power ramp-rates of utility-scale PV systems under passing clouds: Module-level emulation with cloud shadow modelling. Applied Energy, 268, 114980. https://doi.org/10.1016/j.apenergy.2020.114980

[10] Lappalainen, K., Wang, G. C., & Kleissl, J. (2020). Estimation of the largest expected photovoltaic power ramp rates. Applied Energy, 278, 115636. https://doi.org/10.1016/j.apenergy.2020.115636

[11] Shivashankar, S., Mekhilef, S., Mokhlis, H., & Karimi, M. (2016). Mitigating methods of power fluctuation of photovoltaic (PV) sources – A review. Renewable and Sustainable Energy Reviews, 59, 1170–1184. https://doi.org/10.1016/j.rser.2016.01.059

[12] Chen, X., Du, Y., Wen, H., Jiang, L., & Xiao, W. (2019). Forecasting-based power ramp-rate control strategies for utility-scale PV systems. IEEE Transactions on Industrial Electronics, 66(3), 1862–1871. https://doi.org/10.1109/TIE.2018.2840490

[13] Femia, N., Petrone, G., Spagnuolo, G., & Vitelli, M. (2004). Perturb and observe MPPT technique robustness improved. In Proceedings of the IEEE International Symposium on Industrial Electronics (Vol. 2, pp. 845–850). https://doi.org/10.1109/ISIE.2004.1571923

[14] Sera, D., Teodorescu, R., Hantschel, J., & Knoll, M. (2008). Optimized maximum power point tracker for fast changing environmental conditions. In 2008 IEEE International Symposium on Industrial Electronics (pp. 2401–2407). https://doi.org/10.1109/ISIE.2008.4677275

[15] D'Souza, N. S., Lopes, L. A., & Liu, X. (2005). An intelligent maximum power point tracker using peak current control. In 2005 IEEE 36th Power Electronics Specialists Conference (p. 172). https://doi.org/10.1109/PESC.2005.1581620

[16] Tafticht, T., Agbossou, K., Doumbia, M. L., & Cheriti, A. (2008). An improved maximum power point tracking method for photovoltaic systems. Renewable Energy, 33(7), 1508–1516. https://doi.org/10.1016/j.renene.2007.08.015

[17] Ahn, J. Y., Park, J. H., & Cho, B. H. (2004). Dual-module based maximum power point tracking control of PV system. In Nineteenth Annual IEEE Applied Power Electronics Conference and Exposition (Vol. 3, pp. 1509–1514). https://doi.org/10.1109/APEC.2004.1296099

[18] Park, J. H., Ahn, J. Y., Cho, B. H., & Yu, G. J. (2006). Dual-module-based maximum power point tracking control of photovoltaic systems. IEEE Transactions on Industrial Electronics, 53(4), 1036–1047. https://doi.org/10.1109/TIE.2006.878330

[19] Jung, Y., So, J., Yu, G., & Choi, J. (2005). Improved perturbation and observation method (IP&O) of MPPT control for photovoltaic power systems. In Conference Record of the Thirty-first IEEE Photovoltaic Specialists Conference (pp. 1788–1791).

[20] Essa, M. E. S. M. (2019). Identification and temperature control for thermal model of a house based on model predictive control tuned by cuckoo search algorithm. In 2019 15th International Computer Engineering Conference (ICENCO) (pp. 144–149). https://doi.org/10.1109/ICENCO48310.2019.9027474

[21] Serhan, M., Karaki, S. H., & Chaar, L. R. (2005). An adaptive perturb and observe maximum power point tracking system for photovoltaic arrays. In International Solar Energy Conference (Vol. 47373, pp. 515–521). https://doi.org/10.1115/ISEC2005-76251